Journal of Integrative Neuroscience, Vol. 7, No. 2 (2008) 271–286

Imperial College Press
www.icpress.co.uk

Research Report

CELLULAR AUTOMATA APPROACH OF TRANSMEMBRANE IONIC CURRENTS

LAURENT PEZARD*

Laboratoire de Neurosciences Intégratives et Adaptatives
Centre National de la Recherche Scientifique
Unité Mixte de Recherche 6149
Université de Provence — Centre St-Charles, Pôle 3C
3 place Victor Hugo, 13331 Marseille Cedex 3, France
laurent.pezard@univ-provence.fr

ANNICK LESNE**

Institut des Hautes Études Scientifiques
35 route de Chartres, 91440, Bures-sur-Yvette, France
lesne@ihes.fr

Received 8 February 2008
Accepted 14 February 2008

Ionic currents across neuron and glial cells membranes lie at the origin of the entire brain electrophysiology. They are the common root of functional brain dynamics and mesoscopic or macroscopic phenomena such as extracellular fields. In particular, they provide the relevant basis to relate cellular electrophysiology and macroscopic dipole models. In order to derive robust features and to envision the multi-scale approaches required to connect the different levels of observation, an essential prerequisite is to have *minimal* model of elementary ionic motions. In this paper, we propose a general cellular automata framework allowing to investigate the distribution of ionic currents in heterogeneous media interspersed with membranes, from which follows the local electromagnetic field.

Keywords: Ionic currents; cellular automata; multi-scale modeling; electrophysiology.

1. Introduction

Ionic currents across neurons and glial cells membranes lie at the origin of the entire brain electrophysiology. Modeling ionic currents at the molecular scale is thus the very first step to bridge electrophysiological processes and integrated descriptions of neurodynamics. Solving this multi-scale problem in its direct (bottom-up) formulation would greatly help to tackle the inverse (top-down) problem of

*Corresponding author.
**Author's permanent address is Laboratoire de Physique Théorique de la Matière Condensée, Université Paris 6, 4 place Jussieu, F-75252, Paris Cedex 05.

unraveling the functional electrophysiological processes underlying a given cognitive or computational brain activity. Such a multi-scale model could also be exploited to investigate the possible biological role of the local electromagnetic field in volume transmission and ensuing cell interactions.

Ionic currents are involved in both the functional neuronal activity, e.g., spikes, and the generation of the extracellular electromagnetic field measured experimentally, e.g., local field potentials (LFP) or the electroencephalogram (EEG). For instance, the EEG is an average macroscopic signal and as such, determining its relationship with cellular physiology requires to integrate ionic currents from the molecular scale to the millimeter scale. Moreover, the EEG originates in the electromagnetic field generated by the ionic currents transverse to the axons or across the extracellular medium and does not directly reflect the computational properties associated with the genesis and propagation of action potentials. The gap between the phenomena measured in the EEG and the brain functional dynamics thus arises yet at the neuronal scale.

In order to tackle this integration across different scales, we have to devise a minimal model, retaining among the richness of molecular details and processes only those involved in collective effects and leading ultimately to an observable impact at macroscopic scale. Other details could of course be essential in other issues, but they appear to be irrelevant degrees of freedom as regards to emergent phenomena. A minimal model would thus be more efficient in large-scale numerical computations, and more relevant insofar as it yields more generic results.

The present paper details the derivation of such a minimal model that reproduces the elementary properties of transmembrane ionic currents of the cellular electrophysiology, with the right level of details. Hence, it provides the relevant numerical framework for robust multi-scale integration. Being discrete in time, space and state variables, a cellular-automata model is well-suited to drastically reduce the number of degrees of freedom involved in cellular electrophysiology, while allowing, at the same time, to take into account the discrete nature of ions and the stochasticity of their motion [6]. In simple situations, its average steady-state behavior should match the standard electrophysiological equations (briefly recalled in Sec. 2). This central step, allowing at the same time to check the model consistency and fit its parameters, is the core of the present paper (Sec. 3). Potentialities of such an approach are discussed in Sec. 4.

2. Bridging Electrophysiology and Dipole Models: The Frame

2.1. *Standard deterministic equations of cellular electrophysiology*

Cellular electrophysiology, for both neurons and glial cells, is based on the ionic exchanges that take place through the cell membrane. It is now acknowledged that they depend upon the presence of transmembrane proteins: *channels* that allow passive transport of ions along the electrochemical gradient and *pumps* that allow

active exchanges against the electrochemical gradient at the cost of ATP hydrolysis. Passive transport has been first described on empirical grounds before the discovery of ionic channels, by considering that ions move across the membrane under the combined effect of diffusion (thermal motion) and electrical forces, and adopting a deterministic "mean-field" description in terms of average ionic concentrations.[a]

Let, V, the electrical potential in x, c_k the concentration of ion k, z_k its valence and u_k its mobility. Within linear response theory, the contribution $\vec{j}_k$ to the total current density $\vec{J} = \sum_k \vec{j}_k$ is given by the combination of Fick law and Ohm law, leading to the *Nernst-Planck equation*:

$$\vec{j}_k = -u_k(\mathsf{R}T\vec{\nabla}c_k + z_k c_k \mathsf{F}\vec{\nabla}V), \tag{2.1}$$

where $D_k = u_k \mathsf{k_B} T$ is the diffusion coefficient for ion k, T the temperature, $\mathsf{k_B}$ the Boltzmann constant, R the perfect gas constant, and F Faraday constant. It amounts to consider the membrane as an effective uniform dielectric system in which ionic mobilities and activities are spatially homogeneous: such a description comes from the homogenization of a system composed of an "impermeable" part (phospholipids) and a "permeable" one (channels). Since the membrane is locally plane, symmetry arguments ensure that only the direction transverse to the membrane is relevant which allows to locally come down to the unidimensional case.

The *equilibrium potential* $\mathcal{E}_k$ of the ions k is defined as the difference of potential $[V_i - V_e]$ across the membrane at equilibrium for the ions k, that is, when $j_k = 0$. Integration of Eq. (2.1) in such conditions yields the *Nernst equation*:

$$\mathcal{E}_k = -\frac{\mathsf{R}T}{z_k \mathsf{F}} \ln\left[\frac{c_{k,i}}{c_{k,e}}\right], \tag{2.2}$$

where i labels the intracellular compartment and e the extracellular compartment.

Intracellular and extracellular compartments contain different kinds of ions, mainly Na^+, K^+, Cl^- and Ca^{2+}. It is possible to obtain from Eq. (2.1) the *resting potential*, namely the value V_m of the transmembrane potential difference at equilibrium, i.e. when the total current density $\vec{J} = 0$:

$$V_m = \frac{\mathsf{R}T}{\mathsf{F}} \ln\left(\frac{P_{\mathrm{K}}[\mathrm{K}]_i + P_{\mathrm{Na}}[\mathrm{Na}]_i + P_{\mathrm{Cl}}[\mathrm{Cl}]_e}{P_{\mathrm{K}}[\mathrm{K}]_e + P_{\mathrm{Na}}[\mathrm{Na}]_e + P_{\mathrm{Cl}}[\mathrm{Cl}]_i}\right), \tag{2.3}$$

where the contribution of calcium ions has been neglected. This expression is known as the *Goldman-Hodgkin-Katz equation* [4, 5]. V_m differs from the ion equilibrium potentials $\mathcal{E}_k$, hence when $V = V_m$, individual current densities $\vec{j}_k$ do not vanish.

An obvious consistency requirement of stochastic cellular automata model at the ions level will be to recover, on the average, the acknowledged deterministic equations when considering a similar condition, namely two compartments (i.e. intracellular and extracellular compartments), with fixed ionic concentrations separated by a semi-permeable membrane. The interest of such a model will be to reproduce

[a]This point will be of importance in matching this field-theoretic modeling with a more microscopic, discrete and stochastic one in Sec. 3.

the actual distribution of ionic currents, in the complex multi-cellular geometry of the brain tissue, without handling a huge number of coupled equations. Moreover, cellular automata models take into account the discrete nature of ions and the stochasticity of their motion, that are nonnegligible since ionic currents are weak.[b] This distribution expressed at the proper coarse-grained scale may thus be used to substantiate a dipole model and compute the electromagnetic field as recalled in the next subsection.

2.2. *Maxwell equations and the dipole model*

At a mesoscopic scale where a continuous-medium approximation is valid, the electromagnetic field is ruled by Maxwell equations:

$$\vec{\nabla} \cdot \vec{E} = \rho/\epsilon, \tag{2.4}$$

$$\vec{\nabla} \wedge \vec{B} = \mu_0 \vec{J}, \tag{2.5}$$

$$\vec{\nabla} \cdot \vec{B} = 0, \tag{2.6}$$

$$\vec{\nabla} \wedge \vec{E} = 0, \tag{2.7}$$

obtained under several simplifying assumptions: (i) the permeability of the brain tissues is equal to the vacuum permeability μ_0; (ii) the field-induced observables are proportional to the fields (linear response theory); in particular, the polarization writes $\vec{P} = \epsilon_0 \chi_e \vec{E}$ where χ_e is the electrical susceptibility of the medium, from which follows that $\epsilon = \epsilon_0(1 + \chi_e)$; (iii) a quasi-stationary approximation is valid, that amounts to ignore the source terms $\partial\vec{E}/\partial t$ and $\partial\vec{B}/\partial t$ respectively in Eq. (2.5) and Eq. (2.7). The latter Eq. (2.7) implies that it exists a scalar field V (the electric potential) such that $\vec{E} = -\vec{\nabla}V$. The total density of current $\vec{J}(\vec{r})$ can thus be decomposed into [7]:

$$\vec{J}(\vec{r}) = \vec{J_p}(\vec{r}) + \sigma(\vec{r})\vec{E}(\vec{r}) = \vec{J_p}(\vec{r}) - \sigma(\vec{r})\vec{\nabla}V, \tag{2.8}$$

where $\vec{J_p}$ is the primary current and $\vec{E}$ the electric field that it generates. Invoking the absence of charge accumulation at the considered space and time scales, namely $\partial\rho/\partial t = 0$, and assuming $\sigma = cste$, Eq. (2.8) yields:

$$\vec{\nabla} \cdot \vec{J_p} = \sigma \Delta V, \tag{2.9}$$

Eq. (2.9) is the analog of a *Poisson equation* for describing a medium presenting a bulk density of currents generators described by $\vec{J_p}$. Such an "active" medium is fundamentally different from dielectric media encountered in physics and is in fact specific to "living matter". The primary current $\vec{J_p}$ is due to ionic currents generated by neuronal activity, basically currents in ionic channels across cell membranes.

[b]For example, one ion with $|z_k| = 1$ crossing a surface of $1\,\mathrm{mm}^2$ in $1\,\mathrm{ms}$ is responsible for a current of $160\,\mathrm{pA}$, or equivalently, the number of ions with valence z crossing a surface $S\,(10^{-6}\,\mathrm{m})$ in a time $t\,(10^{-3}\,\mathrm{s})$ for a current density $j\,(10^{-12}\,\mathrm{A})$, i.e., jSt/ze, is of the order 10^{-2}.

In the dipole model, the primary current is represented via a superposition of current dipoles $\mathbf{Q}$ each giving a contribution $\mathbf{Q}\delta(\vec{r} - \vec{r}_Q)$ where $\delta(-)$ is the Dirac-delta function. The knowledge of the primary current thus reduces to the knowledge of a dipole distribution. Such a dipole model can be implemented at different scales: for instance, the dipole representation used for interpreting EEG represents cortical activity at millimeter scale, whereas the "physiological" dipoles associated with ionic currents across membranes lie at the nanometer scale. One main aim of our numerical approach is to settle the departure from a precisely tuned building-block allowing to bridge these two representations of the electromagnetic field at far different scales.

3. Bridging Electrophysiology and Dipole Models: The Model

3.1. *Aim and principles*

We present here the design of a numerical framework allowing to articulate electrophysiology and dipole models, in realistic geometries. The challenge is to bridge two field-theoretic deterministic models, at different scales, relying on a different degree of homogenization. We have seen (Sec. 2) that the purely diffusive motion of ions in extracellular and intracellular spaces is strongly affected by the presence of the membrane, across which they experienced both a resistance[c] and a deterministic drift.[d]

We have adopted a cellular automata model which have already been used to account for spatial buffering and diffusion processes in the brain [3, 9]. The model is two-fold: first, a one-dimensional set of nodes represents the physical space and second, particles representing the ions are allowed to move stochastically between nodes. Membrane properties will be modeled at the node level: resistance will be mimicked by a partial reflection of ions on the membrane and the drift by asymmetric laws of motion across the membrane.

We explain here the construction and implementation of a one-dimensional model with a single ionic species, and only mention the additional technicalities required to extend it to dimension 2 or 3 and to several species.

3.2. *Basic dynamic rules*

We have implemented a cellular automata in discrete time ($t = m\tau, m \in \mathbb{Z}$) and space ($x = l\lambda, l \in \mathbb{Z}$), with a formulation suited to perform parallel iterations [2]. The structure of the model and the notations are represented in Fig. 1.

We define two Boolean processes $n_+(x,t)$ and $n_-(x,t)$ which represent the occupation of edges between the successive sites along the array. If a particle arrives in x at time t from $(x - \lambda)$ (i.e., according to the direction $\vec{e}_+$) then $n_+(x,t) = 1$, and

[c]Only a fraction of the membrane is permeable, through ionic channels.
[d]The drift is generated by the electro-chemical gradient actively sustained by ATP-consuming pumps.

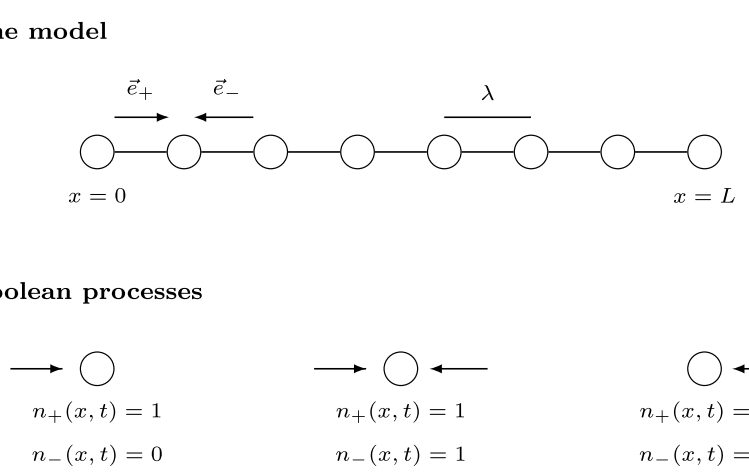

Fig. 1. Representation of the model and notations. Boolean processes $n_\pm(x,t)$ account for the particle motions arriving in site x at time t.

similarly if a particle arrives in x at time t from $(x+\lambda)$ (i.e., according to the direction $\vec{e}_-$) then $n_-(x,t) = 1$ (Fig. 1).

A stochastic motion is obtained by shuffling the direction of motion independently at each site and time. This shuffling is implemented by introducing independent Boolean variables $\mu_\pm(x,t)$, so that the automaton dynamics writes:

$$\begin{aligned} n_+(x+\lambda, t+\tau) &= \mu_+(x,t)n_+(x,t) + [1-\mu_-(x,t)]n_-(x,t), \\ n_-(x-\lambda, t+\tau) &= [1-\mu_+(x,t)]n_+(x,t) + \mu_-(x,t)n_-(x,t). \end{aligned} \tag{3.10}$$

It means that the particle arriving in $x+\lambda$ at time $t+\tau$ according to the direction e_+ (i.e., $n_+(x+\lambda, t+\tau) = 1$) is either a particle that crossed the site x (i.e., that arrived in x at time t from $x-\lambda$ if $\mu_+(x,t) = 1$), or a particle that changed its direction in x (i.e., that arrived in x at time t from $x+\lambda$ if $\mu_-(x,t) = 0$). In other words, $\mu_\pm(x,t) = 0$ prescribes a reflection in x at time t of particles arriving in x along the direction $e_\pm$, and this occurs with a probability $1 - p_\pm(x,t)$.

In the simulations presented here, we considered an array of finite size L with reflecting boundary conditions. At the left border ($x = 0$) this corresponds to:

$$\text{for all } t, \quad n_+(0,t) = 0 \quad \text{and} \quad \mu_-(0,t) = 0, \tag{3.11}$$

(no entry and full reflection) and at the right border ($x = L$) to:

$$\text{for all } t, \quad n_-(L,t) = 0 \quad \text{and} \quad \mu_+(L,t) = 0. \tag{3.12}$$

These conditions ensure that currents vanish at the boundaries (i.e., $j(0,t) = 0$ and $j(L,t) = 0$ for all t) which enforces the system relaxation towards a diffusion equilibrium state. The well-known characteristics of diffusion equilibrium can be compared to the simulation results, providing both a consistency check of the model and a way to fit its parameters. Note that if we consider several ionic species k, the

state variables $n_\pm(x,t)$, the shuffling variables $\mu_\pm(x,t)$ and the associated shuffling parameters $p_\pm(x,t)$ all depend on k.

3.3. *Parameter tuning from free diffusion results*

Free diffusion is implemented with an homogeneous, stationary and symmetric probability $p_\pm(x,t) \equiv p$, i.e., a single shuffling parameter p. Expected features of the diffusion equilibrium are a centered diffusive motion, namely $\langle x_t - x_0 \rangle = 0$ and $\langle [x_t - x_0]^2 \rangle \sim 2Dt$ at short times, before saturation due to the finite size of the domain sets in; then a relaxation towards a diffusive equilibrium with $\langle [x_t - x_0]^2 \rangle = L^2/12$ should occur[e] (Fig. 2). We checked in parallel that the empirical average $\langle x_t - x_0 \rangle$ (average of $x_{t+s} - x_s$ along the simulated trajectory i.e., over s) remains close to 0, never exceeding λ. We also checked that the mean-square-displacement estimate is independent of x_0 (for long enough runs) as expected since we average a sum of increments. We choose $x_0 = L/2$ in all runs of the simulation so as to check the relaxation of an initially localized distribution $\delta(x - L/2)$ towards the uniform distribution in $[0, L]$ corresponding to a diffusive equilibrium (Fig. 3).

A mean-field approach of the large-scale behavior of the automaton allows to relate the diffusion coefficient D of the particles with the parameters of the free-diffusion model according to [2]:

$$D(p) = \frac{\lambda^2}{\tau} \left(\frac{p}{2(1-p)} \right). \tag{3.13}$$

Note that $D(p)$ is a monotonously increasing function of p at fixed λ and τ. An infinite number of triplets (λ, τ, p) allow to fit a given experimental value of the diffusion coefficient D. For instance, once the elementary time and space scales τ and λ are chosen, using some experimental or external arguments, the measured coefficient D is reproduced by choosing $p = 2\tau D/(\lambda^2 + 2\tau D)$. Varying p allows to scan different values of D at fixed time and space scales, i.e., to reproduce within a *unique model* the diffusion behavior of various species in various media. If the diffusion coefficient is known, a change in p should be accompanied by a change in τ and corresponds to changing the minimal time scale of the description (Fig. 4).

3.4. *Parameter tuning from results for a single membrane*

To account for the resistance of a membrane in $x = m$ and its influence on ion motions, the particles should be more likely to change direction at the membrane than in sites of the bulk intracellular or extracellular media, i.e., $\mu_\pm(m,t)$ should take the value 1 with a probability $\tilde{p}_\pm(m) = p/\tilde{r}_\pm(m)$ lower than p. To account for the drift generated by the electric field across the membrane, the parameter

[e]Note that the best estimate of the mean-square-displacement is obtained by an average of $(x_{t+s} - x_s)^2$ along the simulated trajectory (i.e., average over time s); indeed, in this case where $\langle x_t - x_0 \rangle = 0$ from symmetry arguments, subtracting its (non exactly vanishing) empirical estimate in $x_{t+s} - x_s$ would increase the error bar on the mean-square-displacement estimate.

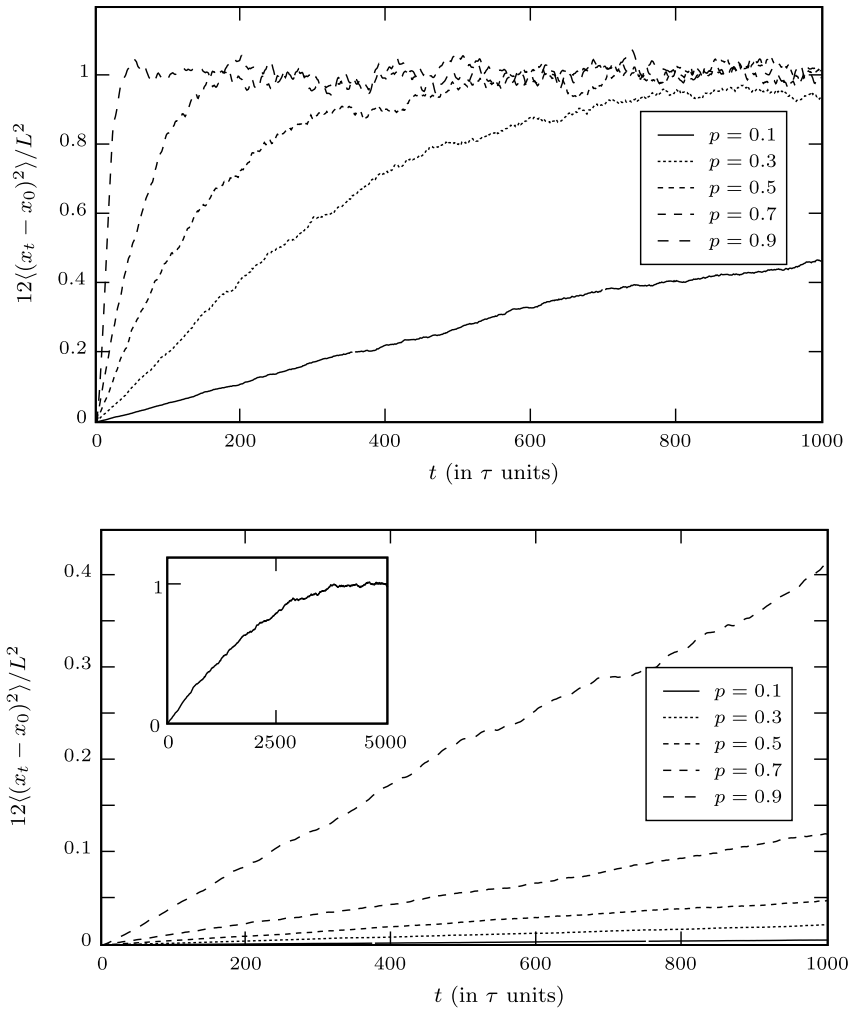

Fig. 2. Diffusive motion of a single ionic species in a domain $L = 50$ (top) or $L = 500$ (bottom) for different values of the shuffling parameter p, represented by plotting the mean-square-displacement $\langle[x_t - x_0]^2\rangle$ as a function of the time t, in units such that $\lambda = 1$ and $\tau = 1$. As expected, finite-size saturation is observed, the faster the larger the diffusion coefficient $D(p)$ is (hence the larger p is) since the crossover time scales as $t_c \sim 1/D(p)$, and the smaller the length is, since $t_c \sim L^2$. We actually plot the dimensionless ratio $12\langle[x_t - x_0]^2\rangle/L^2$ that converges to 1 for a normal diffusive motion in a bounded domain $[0, L]$. Inset shows the convergence to diffusion equilibrium for longer time for $p = 0.9$ and $L = 500$.

$\tilde{r}_{\pm}(m)$ representing the membrane resistivity will take a different value according to the crossing direction. From a physiological viewpoint, we shall distinguish the resistivity $r_i \gg 1$ experienced by a particle coming from the intracellular medium and $r_e \gg 1$ for a particle coming from the extracellular medium. If the left side of the membrane is the intracellular medium and the right side the extracellular medium, $\tilde{r}_+(m) = r_i$ hence $\tilde{p}_+(m) = p/r_i \ll p$ and $\tilde{r}_-(m) = r_e$ hence $\tilde{p}_-(m) = p/r_e \ll p$. The parameter $A = r_e/r_i$ quantifies the bias imposed by the electric field on the diffusive

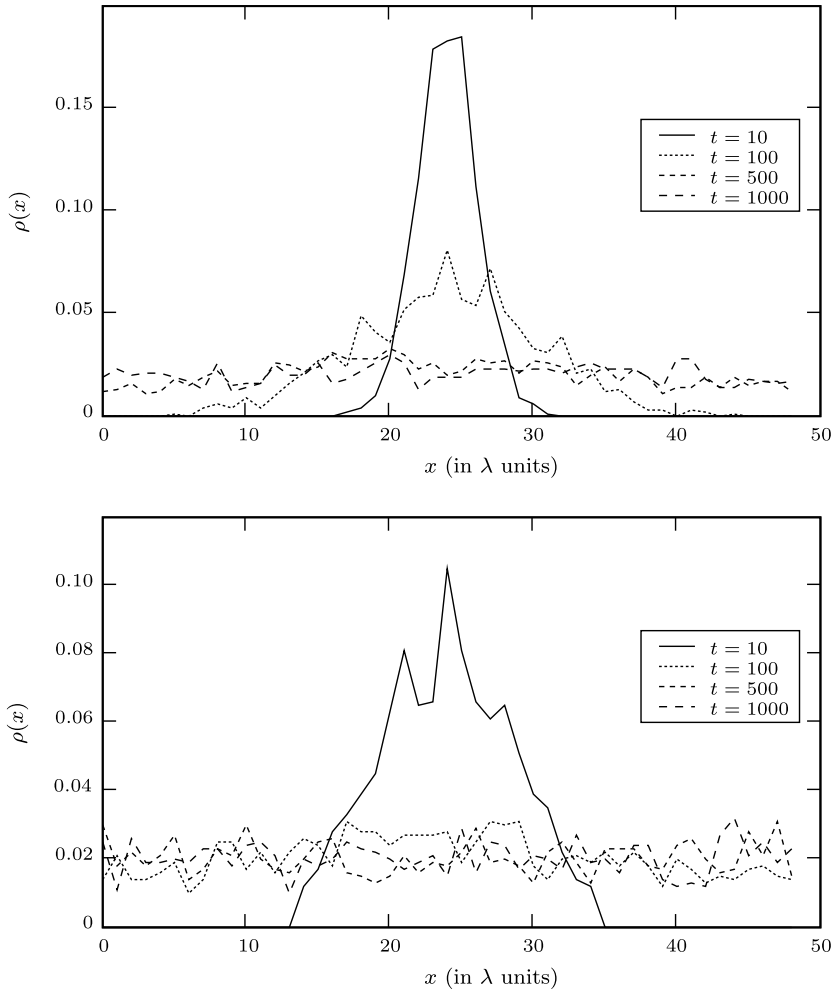

Fig. 3. Time evolution of the density profile $\rho(x)$ in the domain $[0, L]$ with $L = 50$, starting from a point-mass distribution in $x = 25$ (in units where $\lambda = 1$ and $\tau = 1$) for different values of $p : p = 0.3$ (top) and $p = 0.7$, (bottom). The underlying diffusion coefficient $D(p)$ behaves as $p/(1-p)$ hence the equilibration time scales as $t_c \sim (1-p)/p$, we here observe the relaxation to diffusion equilibrium at different levels of stochasticity, the faster relaxation (for $p = 0.7$) being also more stochastic (larger D). A simple scaling argument based on the self-similarity of normal diffusion allows to predict the behavior expected for $L = 500$; numerical check of this behavior (not shown) reinforced our confidence in the relevance of the model and proper tuning of its parameters.

motion inside a ionic channel of the membrane and simply amounting, seen from outside, as a different resistivity according to the crossing direction. The reflective boundary conditions, ensuring that the current vanishes in $x = 0$ and $x = L$, now express $\mu_-(x = 0, t) = 0$ and $\mu_+(x = L, t) = 0$ together with $n_+(x = 0, t) = 0$ and $n_-(x = L, t) = 0$ for all t (hence $\mu_+(x = 0, t)$ and $\mu_-(x = L, t)$ play no role). The relevance of these boundary conditions is their consistency with an equilibrium state, whose characteristics are well known according to the Nernst equation (2.2).

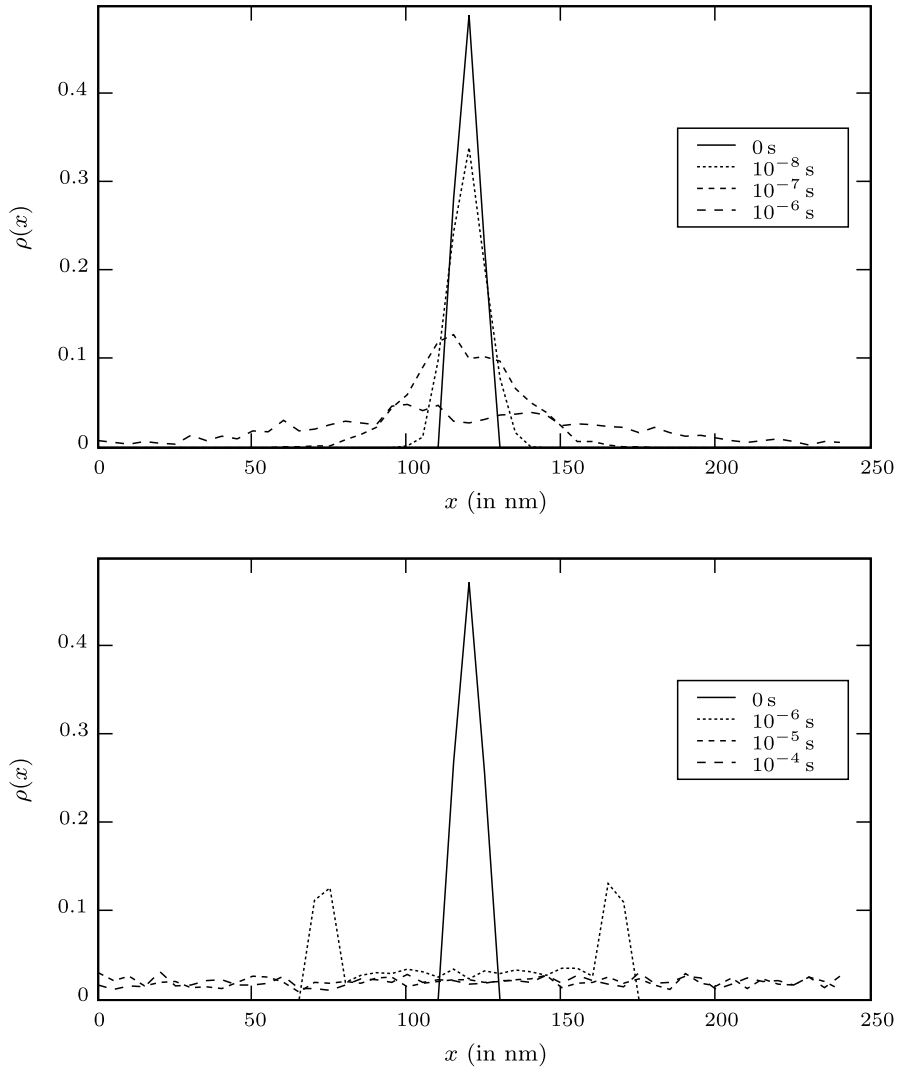

Fig. 4. Same representation as in Fig. 3 but with constant $D = D_{\mathrm{Na}^+} = 1.334 \cdot 10^{-9}\,\mathrm{m}^2 \cdot \mathrm{s}^{-1}$ and $\lambda = a = 5 \cdot 10^{-9}$ m. For each value of τ, the probability p is chosen adaptively: for $\tau = 10^{-9}$ s, $p \approx 9.64 \cdot 10^{-2}$ (top) and for $\tau = 10^{-7}$, $p \approx 99.07 \cdot 10^{-2}$ (bottom). The plots thus present the relaxation to diffusion equilibrium at increasing time scale.

As in the case of free diffusion, we have to tune the additional two parameters r_e and r_i by comparing numerical prediction with the experimentally observed behavior. The current across the membrane writes $j(x = m, t) = (\lambda/\tau)[\mu_i(m,t)n_i(m,t) - \mu_e(m,t)n_e(m,t)]$, hence the average current is:

$$\langle j(m,t)\rangle = \frac{\lambda}{\tau}(\langle\mu_i(m,t)\rangle\langle n_i(m,t)\rangle - \langle\mu_e(m,t)\rangle\langle n_e(m,t)\rangle), \tag{3.14}$$

where the average is over the stochasticity generated by the random shuffle (we have here used the statistical independence of $\mu_\alpha(x,t)$ and $n_\alpha(x',t')$ for any x, x'

and $t' \leq t$). Since only a very small fraction of ions crosses the membrane, the ensuing asymmetry in the ionic movement directions can be neglected and the bulk fraction of ions going to the left identified with the bulk fraction of ions going to the right. Assuming for definiteness that the left compartment is intracellular, it follows that

$$\langle n_-(m,t)\rangle = \langle n_+(m-1,t)\rangle = c_i/2 \quad \langle n_+(m,t)\rangle = \langle n_-(m+1,t)\rangle = c_e/2. \quad (3.15)$$

Using the average values $\langle \mu_i \rangle = p/r_i$ and $\langle \mu_e \rangle = p/r_e$, the average current density: $J = z\mathsf{F}\langle j \rangle$ writes $J = (pz\mathsf{F}\lambda/2\tau)(c_i/r_i - c_e/r_e)$. The equilibrium $J = 0$ is obtained for $(c_e/c_i)_{eq} = r_e/r_i = A$, hence, comparison with Nernst equation (2.2) gives:

$$A = e^{z\beta e\mathcal{E}} \quad \text{or} \quad A = e^{z\mathsf{F}\mathcal{E}/\mathsf{R}T}. \quad (3.16)$$

The equilibrium potential thus fully prescribes r_e and r_i. In other words, we encapsulate in r_e and r_i either the experimental knowledge of the equilibrium potential, or the (constant) values of the ionic concentrations on each side of the membrane in steady state.

Note that λ and τ are not directly related to the membrane thickness and crossing time: the latter are encapsulated in the parameters p, r_i and r_e, so that the membrane influence on ions motion is fully accounted in this effective way, involving a single site $x = m$ with no width and no explicit delay. The model thus allows to compute ionic currents at different space and time resolution. For instance, we might take λ equal to the actual membrane thickness $a \approx 5\,\text{nm}$ but consider in the simulation that the membrane is point-wise located in $x = m$, except in devising the geometric setting of the simulation: the overlap of the membrane with cells $[m-1, m]$ and $[m, m+1]$ should be taken into account when prescribing the size of the array and location of other membranes or boundaries. Since we aim at predicting emergent phenomena, we shall also be interested in mesoscopic simulations with $\lambda \gg a$ and $\tau \gg a^2/2D$, possibly fed in a hierarchical way with the results of a smaller-scale simulation.

Starting from an homogeneous ionic distribution in the intracellular and extracellular compartments, we checked the expected convergence towards an *asymmetric* distribution as prescribed through the asymptotic relation $(c_e/c_i)_{eq} = A$ (Fig. 5). In all tested cases, the concentration ratio c_e/c_i converges toward A (Fig. 6). This feature supports the consistency of our effective model and the proper physiological interpretation of the parameter A. Investigating the time evolution of the density profile shows that the parameters r_e and r_i slow down the transit of the ions from one compartment to the other; accordingly, they are directly related to the equilibration time, the relaxation to the equilibrium state being slower for larger values (Fig. 7). Membrane crossings are rare events. The presence of the membranes thus induces a considerable change of time scale between the fast "physical" and individual ionic motions, and their slow collective and "physiological" consequences, at the millisecond scale.

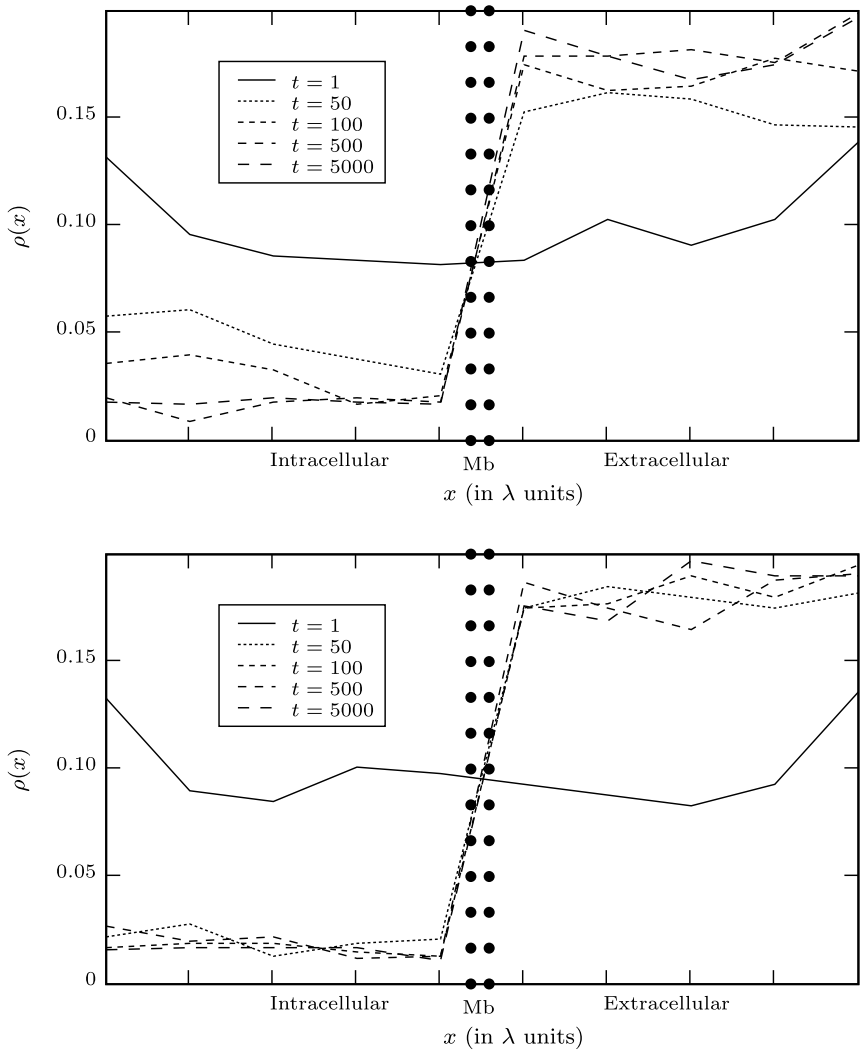

Fig. 5. Time evolution of the density profile for $A = 10$ at fixed units $\lambda = 1$ and τ, with $p = 0.3$ (top), $p = 0.7$ (bottom). In what follows, we considered a system with length $L = 9$ in which the middle site is the membrane. Since the extracellular space is about 25 nm, the five intervals on one side of the membrane represent the extracellular compartment (at the right scale); the other side of the membrane can be considered as a part of the intracellular compartment. In both compartments, the movements of the ions are correctly described as normal diffusion ($r_e = r_i = 1$). Furthermore, if $D = 2 \cdot 10^{-5}\,\mathrm{cm^2\,s^{-1}}$ is given it corresponds approximatively to the diffusion coefficient of K^+ or Cl^- ions in aqueous solution [1], one obtains $\tau \sim 10^{-9}\,\mathrm{s}$ for $p = 0.3$ and $\tau \sim 10^{-8}\,\mathrm{s}$ for $p = 0.7$.

These observations are the numerical validation of our model consistency, since it properly recovers the ionic concentration differences that have been used in fixing the values of the parameters r_e and r_i. This numerical consistency supports the fact that ion dynamics across the membrane can indeed be captured by such a minimal cellular automata model.

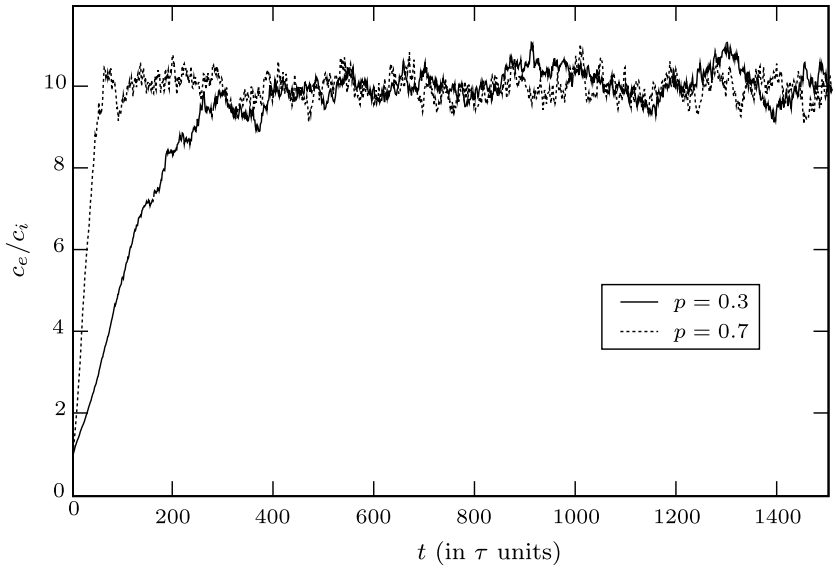

Fig. 6. Time evolution of the concentration ratio $c_e(t)/c_i(t)$ for $A = 10$. We check the asymptotic convergence of this ratio towards $c_{e,eq}/c_{i,eq} = A$.

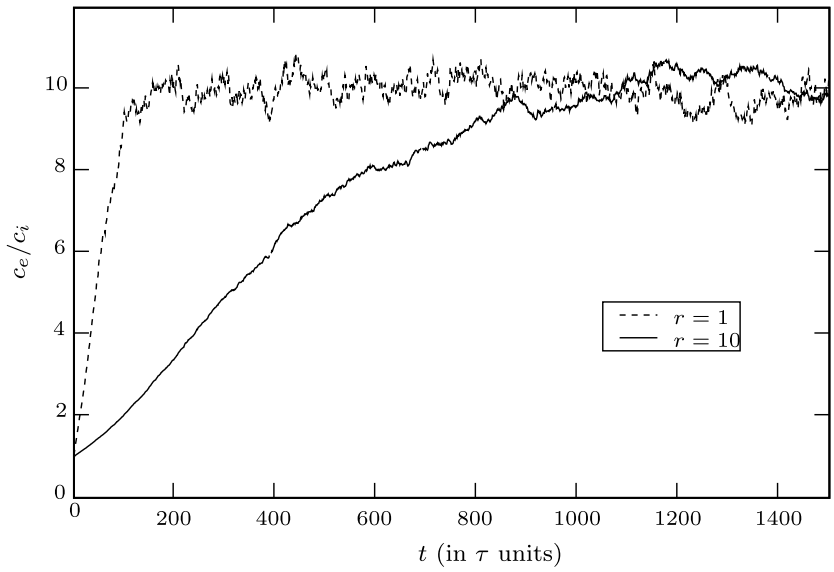

Fig. 7. Time evolution of the concentration ratio for $r_e = r_i = 1$ and $r = 10$ with $A = 10$ and $p = 0.5$. We check here the slowing down induced by the membrane.

3.5. *Implementation in more complex situations*

In principle, our cellular automaton straightforwardly extends to the case of a medium with several membranes, several ionic species, in dimension 2 or 3, at various scales. It thus provides a flexible framework to simulate brain tissue from

the molecular scale to the scale of cell populations. Let us just mention an example and a few guidelines to achieve its extended implementation.

It is first possible to account for different diffusion coefficients in the intracellular and extracellular compartments by taking $p_i \neq p_e$. Our numerical model is thus naturally suited to simulate heterogeneous media with a space-dependent diffusion coefficient $D(x)$, simply by considering a space-dependent shuffling parameter $p(x)$ such that $D[p(x)] = D(x)$. Integration of the simulation results then gives a direct access to the emergent large-scale behavior, thus avoiding the (much difficult) auxiliary computation of an homogenized diffusion coefficient that is required to come down to a tractable effective diffusion equation [8].

Another basic extension is to consider several ionic species k diffusing jointly. In this case, p, r_i and r_e (hence A) depend on k. Although the different ions do not directly interact, the membrane potentials depend jointly on all ionic species (Goldman-Hodgkin-Katz equation (2.3)), hence, couple them since a change of concentration in any of those species will affect the diffusion of all the other ones. This is one of the basic electrophysiological principles, and it is exploited in several ways, for instance the modification of the fixed ions concentrations, the control of the pumps activity or spatial buffering.

Considering a 1D array of membranes is enough to appreciate, at the still moderate scale of several cells, the cumulative effect of membranes on the ionic currents in one direction (that of the array), provided it is valid to assume the homogeneity and symmetry in transverse directions ensuring the absence of any leak or input currents. The 1D-simulation is implemented by placing k membranes on sites $x = m_j$, $j = 1, \ldots, k$. The sites $(m_j)_j$ could be placed regularly, for simplicity, or randomly placed according to a physiologically more relevant distribution. It is important to note that, when following the array in one direction, the membranes will be alternatively between the extracellular medium (on the left of the membrane) and an intracellular medium (on the right) for j odd, and conversely for j even. Figure 8 gives a simple example of the situation where a neuron is separated from a glial cell by an extracellular compartment. Realistic parameters are used to deal with Na^+ and K^+ and their different permeabilities. The heterogeneous equilibrium which is reached by the simulations gives coherent values for equilibrium potentials for each ion and each type of cell ($\mathcal{E}_{\mathrm{Na}} = 58\,\mathrm{mV}$ and $\mathcal{E}_{\mathrm{K}} = -92\,\mathrm{mV}$ for the neuron compartment; $\mathcal{E}_{\mathrm{Na}} = 66\,\mathrm{mV}$ and $\mathcal{E}_{\mathrm{K}} = -83\,\mathrm{mV}$ for the glial compartment). This result would be easily extended to more cellular compartments.

At larger scale, current loops might settle and evidently require a genuinely 2D or 3D model. To efficiently model the brain tissue at such a larger scale, it is relevant to repeat the coarse-graining and homogenization process used in the previous sections to design our minimal model at a supra-molecular scale. In practice, it amounts to consider a cellular automaton model, with a lower resolution $\lambda' > \lambda$, $\tau' > \tau$, i.e., to consider more integrated "elementary" steps. The preliminary 1D study at resolution (λ, τ), will then provide the effective parameters for the higher-level model at resolution (λ', τ').

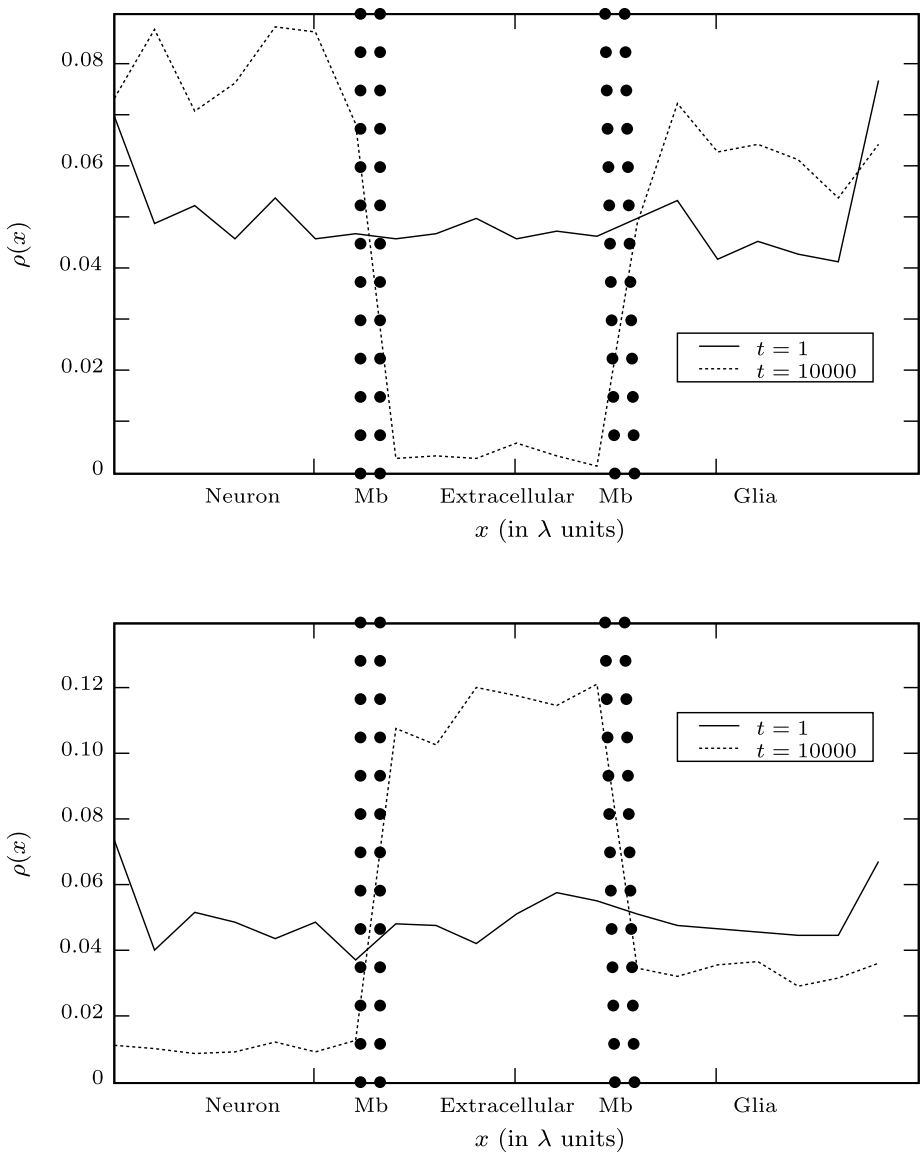

Fig. 8. An example of results using two membranes and realistic parameters for K^+ (top) and Na^+ (bottom). The parameters were: $\lambda = 5 \cdot 10^{-9}$ m, $\tau = 0.1 \cdot 10^{-3}$ s, $D_{\mathrm{K}} = 1.957 \cdot 10^{-9}\,\mathrm{m}^2 \cdot \mathrm{s}^{-1}$, $D_{\mathrm{Na}} = 1.334 \cdot 10^{-9}\,\mathrm{m}^2 \cdot \mathrm{s}^{-1}$. In the case of K^+, the parameters of the neuron membrane are: $r_- = 1$ and $r_+ = 25$ and the parameters of the glial membrane were: $r_- = 20$ and $r_+ = 1$. In the case of Na^+, the parameters of the neuron membrane were: $r_- = 25$ and $r_+ = 2.5$ and the parameters of the glial membrane were: $r_+ = 2500$ and $r_- = 625$.

4. Conclusion

Our cellular automata approach provides an agent-based numerical model simple and efficient enough to achieve multi-scale integration in arbitrary geometries. Its novelty is first to involve membranes and focus on their role and second to aim

at computing the dipoles of currents. It has shown that the membrane tends to slow down and localize electrical activity. On the basis of its discrete and stochastic characteristics, this approach also allows to investigate the impact and biological role of fluctuations arising in the ionic transport across the cell membranes. Its variables and parameters exploit our knowledge of elementary electrophysiological mechanisms. More precisely, the parameters (p and $r_{\pm}$) can be either computed from precise experimental values of the steady-state ionic concentrations, either chosen together with the geometry between several generic alternatives, or determined self-consistently by completing the actual model of ionic channels with the effective action of pumps. In this latter case, the values of the concentrations will be related to the kinetic parameters of the pumps, their density and the ATP flux fueling them. Note that the contribution of fixed ions to the difference of potential (i.e., Donnan equilibrium) can be easily included. Two extra global parameters λ and τ prescribe the space and time resolution of the overall description and are supplemented with the geometry and location of membranes.

The outcome of this model, i.e., the description of ionic currents distribution at different scales according to the functional state of the neurons, is a first step in the hard task of unraveling dynamic processes and functional mechanisms underlying experimental records. Beyond establishing the connection between dipole models at different scales, this numerical framework could be exploited to address central questions like lateral interactions between neurons or between neurons and glial cells, and buffering effects in the extracellular medium.

References

[1] Chen KC, Nicholson C, Spatial buffering of potassium ions in brain extracellular space, *Biophys J* **78**:2776–2797, 2000.

[2] Chopard B, Droz M, *Cellular Automata Modelling of Physical Systems*, Cambridge University Press, Cambridge, UK, 1998.

[3] Dai L, Miura RM, A lattice cellular automata model for ion diffusion in the brain-cell microenvironment and determination of tortuosity and volume fraction, *SIAM J Appl Math* **59**:2247–2273, 1999.

[4] Goldman DE, Potential impedance, and rectification in membranes, *J Gen Physiol* **27**(1):37–60, 1943.

[5] Hodgkin AL, Katz B, The effect of sodium ions on the electrical activity of the giant axon of the squid, *J Physiol* **108**:37–77, 1949.

[6] Lesne A, Discrete vs continuous controversy in physics, *MSCS* **17**:185–223, 2007.

[7] Malmivuo J, Plonsey R, *Bioelectromagnetism — Principles and Application of Bioelectric and Biomagnetic Fields*, Oxford University Press, New York, 1995.

[8] Nicholson C, Diffusion and related transport mechanisms in brain tissue, *RPP* **64**:815–884, 2001.

[9] Steinberg B, Wang Y, Huang H, Miura R, Spatial buffering mechanism: Mathematical model and computer simulations, *Math Biosci Eng* **1**:1–28, 2005.